Dynamic WPT Transmitting Through Fiber-Belt Tire and CFRP Wheel to In-Wheel Arc-Shaped Coil

Osamu Shimizu, *Member, IEEE,* Takashi Utsu, *Student Member, IEEE,* Hiroshi Fujimoto, *Senior Member, IEEE,* Daisuke Gunji, *Member, IEEE,* and Isao Kuwayama

***Abstract*—Dynamic wireless power transfer (WPT) can solve the short cruising range problem of electric vehicles, moreover it makes electric vehicles more efficient due to reducing heavy battery of electric vehicles. However to be reduced receiving energy of dynamic WPT by foreign matter objects is one of the major problems of dynamic WPTs. Prevention of the entry of foreign objects between the transmitter and receiver coils is the best method to increase opportunity WPT and energy of WPT. This paper aims to propose a new WPT system named in-wheel coil, which can prevent foreign objects by power transfer through tire and wheel, and also proposes its suitable materials and design. The non-metal materials of wheels and tires for the proposed system are evaluated by actual measurement with small evaluation equipment, hence the suitable materials which decrease WPT efficiency hardly are proposed. The proposed system is also evaluated by full-scale model with power transfer test. In addition, the mutual inductance model of arc-shaped coil, which can minimize airgap between the transmitter coil and the receiver coil.**

***Index Terms*—Electric vehicles, Wireless power transmission, Production materials, In-wheel Motor, In-wheel Coil**

I. Introduction

ONE of the main obstacles in electric vehicles is the short cruising range. To solve this problem, several dynamic wireless power transfer(WPT) systems [1] - [6], which are breakthrough technology, have been proposed. Dynamic WPT can improve not only cruising range, but also driving efficiency due to reduction of battery weight. Therefore dynamic WPT can reduce 17 % driving loss with 92.5 % of DC-to-DC efficiency [7].

Especially, the unsprung coil [8] is a novel approach to improve efficiency of WPT by minimizing the air gap between a road surface and a receiving coil. The air gap with the road surface coil is kept constant even when the suspension is displaced, and the air gap is minimized. Minimum air gap of body side coil is 100mm which is given by SAE J2954 standard, however the air gap of unsprung coil which can avoid collision against steps of road by moving with tire can be a half of body coil's air gap. Feasibility study is also considered in some locations [9] - [11].

O. Shimizu, T. Utsu and H. Fujimoto are with the Department of Advanced Energy, The University of Tokyo,5-1-5, Kashiwa no ha, Kashiwa city, Chiba 277-8561,Japan(TEL:+81-4-7136-3881, e-mail:osamu.shimizu@edu.k.u-tokyo.ac.jp).

D. Gunji is with Powertrain Tech. Dev. Dept., NSK Ltd.,1-5-50 Kugenuma Shimmei, Fujisawa city, Kanagawa 251-8501,Japan, e-mail:gunji-d@nsk.com)

I. Kuwayama is with the Next Generation Technology Development Dept.1,Bridge Stone Corporation,3-1-1 Ogawa Higashicho,Kodaira city, Tokyo 187-8531,Japan,(e-mail:isao.kuwayama@bridgestone.com)

However, the WPT system also includes certain problems, among which the presence of foreign objects such as small animals or metal pieces between the transmitter and receiver coils is a major issue [12]. This poses risk of damage to the animal or ignition by eddy current loss and is dangerous. Hence, it is necessary to detect foreign objects and stop the transmission or remove such objects. The WPT charging energy is determined by the output, efficiency, and charging time. Therefore, an dynamic WPT system has to detect foreign objects more rapidly than a stationary WPT system because the duration from the WPT start to end is less. An equivalent circuit model [13] for the detection system and detection system have been proposed to solve this problem; however, the fundamental solution involves the prevention of the entry of foreign objects between the coils.

This paper expands on the work presented at the conference [14]. The improvements from the previous work are system evaluation by the power transfer test and evaluation for the materials. This paper aims to propose a WPT system which can prevent foreign objects between the transmitter and receiver coils by transmitting through the tire and the wheel. With proposal of the system, suitable materials of the tire and the wheel are proposed. To provide methodology of calculation for mutual inductance is also aimed. The innovations in this research are shown as below.

1. The new system that can prevent foreign matter objects
2. Calculation model of mutual inductance for the new system
3. Suitable materials for the new system, which are structure of CFRP and belt of tire

II. In-wheel Coil

To prevent the entry foreign objects, we propose to locate the receiver coil within the wheel named in-wheel coil, as shown in Fig. 1. In this system, the location of the tire and wheel between the transmitter and receiver coils prevents the entry of foreign objects therein. The receiver coil is fixed to the case of inverter which is fixed to upright of the suspension, then it does not rotate with the tire. The conventional receiver coil for a wireless in-wheel motor (WIWM) system is located outside the wheel as shown in Fig. 1 and Fig. 2, because the metal wheel and steel belt in the tire are composed of metal, and may cause eddy currents [15]. The metal wheel, in particular, not only causes loss but also functions as a magnetic shield. To address this issue, two solutions are proposed, namely the usage of a wheel composed of carbon fiber reinforced plastic (CFRP) and that of a tire composed of fiber belt.

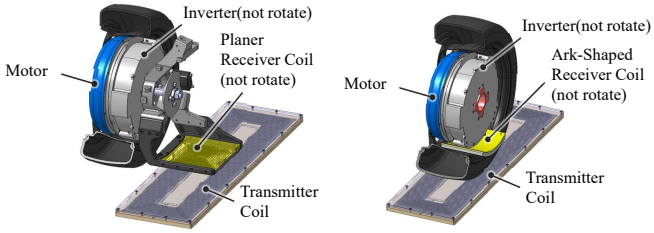

(a)Conventional Coil Layout:The receiver coil is outside of the wheel

(b)Proposed Coil Layout: The receiver coil is inside of the wheel

Fig. 1. Difference of 2 types of Coil Layout

(a)Test Vehicle

(b)System Layout

Fig. 2. Conventional System of WIWM

The differences of 2 types of coil are the receiver coil layout, the receiver coil shape and materials around the receiver coil. The transmitter coil is compatible. Proposed coil layout have to use CFRP for wheel and fibers for tire, then it will cost more than conventional system. On the other hand, CFRP or fiber will be more efficient vehicles due to their lighter weight. Though the shape of the coils is different, manufacturing cost of the receiver coil and assembly the receiver coil are the same due to the same manufacturing process and materials.

III. Mutual Inductance Model of an Arc-shaped Coil

The conventional receiver coil is planer-shaped for minimizing the coil gap. However, this planer-shaped coil air gap is larger, when located within the wheel. Therefore, an arc-shaped coil is proposed to minimize the air gap for the in-wheel motor system, as shown in Fig. 1. Materials or manufacturing process of the arc-shaped is the same as the conventional planer-shaped coil when it is mass produced. The proposed dynamic WPT system uses a series-series (SS) circuit. In SS circuit,the transmission power P_{ac} and the transmission efficiency η are as follows:

$$P_{ac} = \frac{(\omega_0 L_m)^2 R_{ac}}{\left(R_1(R_2+R_{ac})+(\omega_0 L_m)^2\right)^2} V_1^2 \quad (1)$$

$$\eta = \frac{(\omega_0 L_m)^2 R_{ac}}{(R_2+R_{ac})\left(R_1 R_{ac}+R_1 R_2+(\omega_0 L_m)^2\right)} \quad (2)$$

Here, R is the coil resistance, L is the coil inductance, L_m is the mutual inductance, and subscripts 1 and 2 represent the transmitter and receiver sides, respectively. C is the capacitance of the resonance capacitor and R_{ac} is the equivalent load resistance.

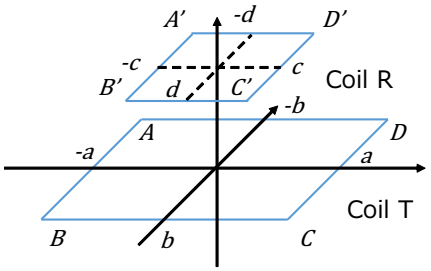

Fig. 3. Coordinates for mutual inductance calculation of rectangular coil

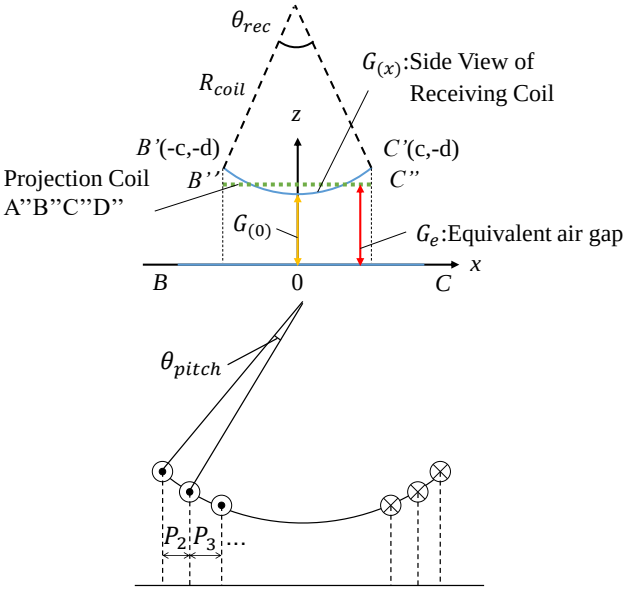

Fig. 4. Coordinates for mutual inductance calculation of arc-shaped coil approximated into rectangular coil model

Therefore, the mutual inductance is an important parameter for calculating the transfer power and efficiency.

The rectangular coils are arranged facing each other as shown in Fig. 3; current flows in coil T, which represents the i-th turn from the inside of the transmission coil, and coil R represents the j-th turn from the inside of the receiving coil. A,B,C,D and A',B',C',D' are points of the edges in the rectangular coils.

The magnetic flux Φ_{CD} passing through coil R, caused by the current flowing in side CD is expressed by the following equation [17]:

$$\Phi_{CD} = \frac{\mu_0}{2\pi}\left[R_{CA'} - (a+c)\text{arctanh}\frac{a+c}{R_{CA'}} - R_{CD'} + (a-c)\text{arctanh}\frac{a-c}{R_{CD'}} - R_{CB'} + (a+c)\text{arctanh}\frac{a+c}{R_{CB'}} + R_{CC'} - (a-c)\text{arctanh}\frac{a-c}{R_{CC'}}\right] \quad (3)$$

Here, $R_{CA'}$ is the distance between points C and A'. $R_{CD'}$, $R_{CC'}$,$R_{CB'}$ are distance between points of subscript the same as $R_{CA'}$. The mutual inductance of coils T and R is

$$M_{ij} = \Phi_{AB} + \Phi_{BC} + \Phi_{CD} + \Phi_{DA}. \quad (4)$$

The total mutual inductance M is considered as the following sum of

$$M = \sum_{i=1}^{N^T} \sum_{j=1}^{N^R} M_{ij} \tag{5}$$

.

Where N^T is number of transmitting coil turns, and N^R is number of receiving coil turns.

The air gap between the arc-shaped and rectangular coils is not constant. Therefore, an equivalent gap is proposed. The equivalent gap G_e depicted in Fig. 4 is expressed by the following equation:

$$G_e = \frac{1}{R_{B''C''}} \int_{-c}^{c} G_{(x)} dx \tag{6}$$

Here, $G_{(x)}$ is vertical distance between the transmitter coil and the receiver arc-shaped coil. $R_{B''C''}$ is the distance between points B'' and C'' which are the points of edge in the arc-shaped coil.

The arc-shaped model is considered as the projected model from the transfer- side. Therefore, the coil pitch is not constant. This coil pitch is expressed by the following equation:

$$P_j = R_{coil}(\cos(\frac{\theta_{rec}}{2}) - \cos(\frac{\theta_{rec}}{2} - \theta_{pitch}(j-1))) \tag{7}$$

. Here, θ_{rec} is the coil angle and θ_{pitch} is the coil pitch angle; P_j is the projection the j-th coil pitch which is the j-th turn from the outside the receiving coil; R_{coil} is the radius of the coil.

The coordinates of the coil can be calculated using Equations(6) and (7). Finally, the mutual inductance is calculated using these coordinates and equations(3), (4), and (5).

IV. Full-Scale Model Design

The target size of the full-scale model is listed in Table I.

The minimum air gap of the arc-shaped coil $G_{(0)_{min}}$ is expressed by the following equation:

$$G_{(0)_{min}} = \frac{D_t - D_{wi} + D_{c1} + D_{c2}}{2} + C_w + T_{c1} + T_{c2} + T_r \tag{8}$$

Here, D_t is the diameter of the tire; D_{wi} is the inner diameter of the wheel; C_w is the clearance between the wheel and coil case necessary for preventing contact; W_c is the thickness of the coil case composed of resin for isolation. The proposed mutual inductance model defines the coil gap as the distance between the coil centers. Therefore, the coil diameters D_c are considered. T_r is the thickness of the road pavement material.

The components that determine the coil gap $G_{(0)_{min}}$ are shown in Fig. 5.

Calculating with the parameters listed in Table I, the full-scale arc-shaped coil's minimum air gap G_0 is 112 mm. To minimize the equivalent gap, the radius of the receiving coil R_{coil} should be as large as possible. Therefore, $R_{coil_{max}}$ is expressed by the following equation, and its value is 223.5 mm for this model.

$$R_{coil_{max}} = \frac{D_{wi} - D_{c2}}{2} - C_w \tag{9}$$

The dimensions of the full-scale coil are depicted in Table. II. The total length of the arc-shaped coil is set to be the same as that of the rectangular one. Two layers of the receiving coil need to be downsized. Litz wire is adopted for the coil to reduce the resistance caused by skin effect.

TABLE I
Parameters of Full-scale Model

Parameter	Value
Diameter of the Tire,D_t [mm]	644
Diameter of the Wheel Rim[mm]	508 (20 inch)
Diameter of the inside of the Wheel,D_{wi}[mm]	464
Clearance between the Wheel and Coil Case,C_w[mm]	5
Thickness of Transmitter Coil Case,T_{c1}[mm]	2
Thickness of Receiver Coil Case,T_{c2}[mm]	2
Diameter of Transmitter Coil,D_{c1}[mm]	3
Diameter of Receiver Coil,D_{c2}[mm]	3
Thickness of the Road Pavement Material,T_r[mm]	10

V. Evaluation of the Full-Scale Model

The evaluation results with LCR meter are displayed in Fig. 6 and Table. III, at a transmitting frequency of 85 kHz.

The error between the calculation and actual measurement is also $\pm 5\%$, similar to that of the one-third model. However, the air gap of the full-scale rectangular coil must be at least 23.8 mm greater than that of the arc-shaped coil because of

TABLE II
Dimensions of the Full-scale Coil

Parameter	Value	
	Transmitter	Receiver
Width of the Coil Center[mm]	250	179.5
Length of the Coil Center[mm]	1000	179.5
Diameter of the Coil[mm]	3	3
Coil Pitch [mm]	6	6
Number of Turns	12	13
Number of Layers	1	2
Width of the Coil Case[mm]	318	230
Length of the Coil Case[mm]	1086	230
Height of the Coil Case[mm]	45	26.5
Wire type	Litz Wire AWG 44x6250	

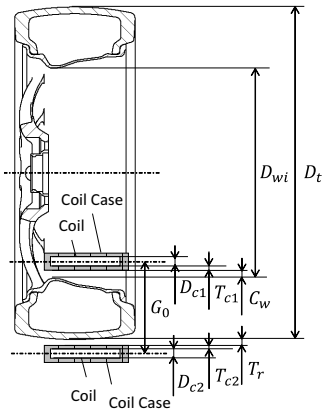

Fig. 5. Parameters for calculation of minimum coil gap

the constraint in setting the rectangular coil within a 225-mm cylinder.

Hence, for comparison at the same conditions, the air-gap of the rectangular coil is 23.8 mm more than that of the arc-shaped coil's minimum air gap. The calculated results are depicted in Figs. 7 and 8, considering the constraint of the coil position. The horizontal axis represents the minimum gap of the arc- shaped coil. The transmission-side power supply voltage V_1 is set 300 V. The difference between the arc-shaped coil and rectangular coil is caused by the larger air gap of the rectangular coil.

Certain metals are present around the receiving coil in the car, causing eddy current loss. Moreover, there are certain regulations on flux leakage. Therefore, it is necessary to consider the formation of a closed magnetic circuit with ferrite, to a certain degree. To form a closed magnetic circuit, ferrite blocks are set behind both coils.

A rectangular ferrite block is divided into small pieces and placed in the arc-shaped ferrite case. This is evaluated using the same experimental equipment used for the coil without ferrite.

The evaluation result is depicted in Table. IV. The maximum coil-to-coil efficiency is verified with the coupling coefficient, k, and quality factor, Q_i. These parameters are expressed by the following equations:

$$k = \frac{L_m}{\sqrt{L_1 L_2}} \tag{10}$$

.

$$Q_i = \frac{\omega_0 L_i}{R_i} (i = 1 \text{ or } 2) \tag{11}$$

Here, ω_0 is the resonant frequency. The theoretical maximum efficiency η_{max} can be calculated using k and Q_i as follows:

$$\eta_{max} = \frac{k^2 Q_1 Q_2}{(1 + \sqrt{1 + k^2 Q_1 Q_2})} \tag{12}$$

The evaluation results demonstrate considerable increase in the inductance as well as resistance, indicating that the flux passes ferrite well. As the result, although the maximum output decreases, the maximum efficiency increases. A maximum coil-to-coil efficiency of 97.7% is achieved theoretically at the nominal position as shown in Fig. 9. In dynamic situation, position of the receiver coil is not only nominal ,then maximum coil-to-coil efficiency with misalignment is evaluated as shown in Fig. 10. Longitudinal position 0mm and misalignment 0mm is the center of the transmitter coil which is the nominal horizontal position of the receiver coil. When the receiver coil position is on the longitudinal position of ±360mm coil-to-coil efficiency is more than 94 % with the lateral misalignment of ±90mm.

WPT performance is verified using the evaluation equipment shown in Fig. 11. DC input of the transmitter and DC

TABLE III
COIL PARAMETERS FOR THE EXPERIMENT

Parameter	Value	
	Rectangular	Arc-shaped
Resistance of the Transmitter Coil[mΩ]	89.3	
Self-inductance of the Transmitter Coil[μH]	157.9	
Resistance of the Receiver Coil[mΩ]	34.7	34.6
Self-inductance of the Receiver Coil[μH]	61.8	60.9

TABLE IV
EXPERIMENTAL RESULTS WITH 112MM AIR GAP AT NOMINAL POSITION

Parameter	Value
Resistance of the Transmitter Coil[mΩ]	152
Self-inductance of the Transmitter Coil[μH]	249
Resistance of the Receiver Coil[mΩ]	35.5
Self-inductance of the Receiver Coil[μH]	95.2
Mutual Inductance[μH]	12.1
Maximum Coil Efficiency η_{max} [%]	97.7

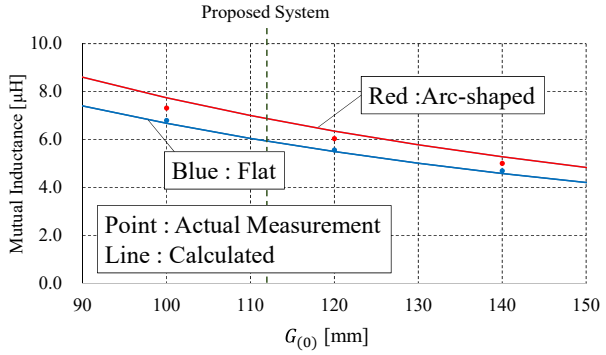

Fig. 6. Gap vs mutual inductance when coil is set in the wheel

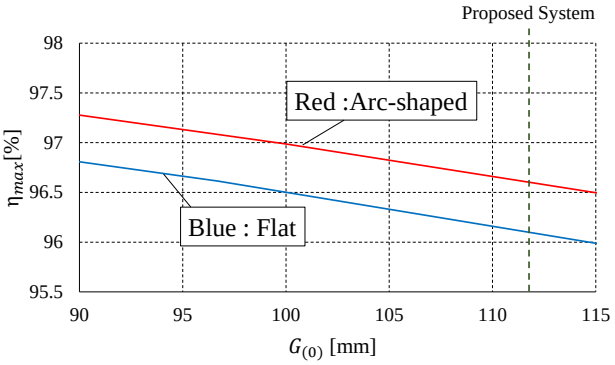

Fig. 7. Minimum gap vs theoretical efficiency when coil is set in the wheel

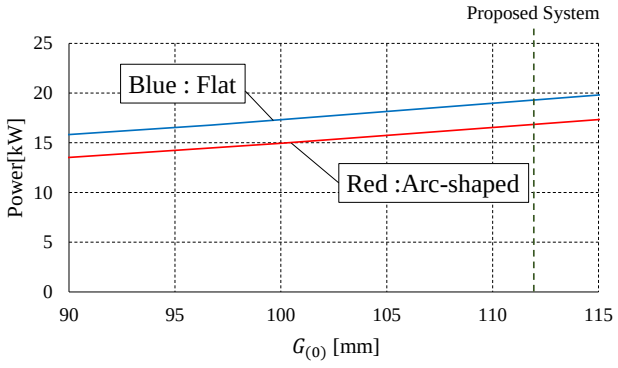

Fig. 8. Minimum gap vs calculated power with $V_1 = 300$ when coil is set in the wheel

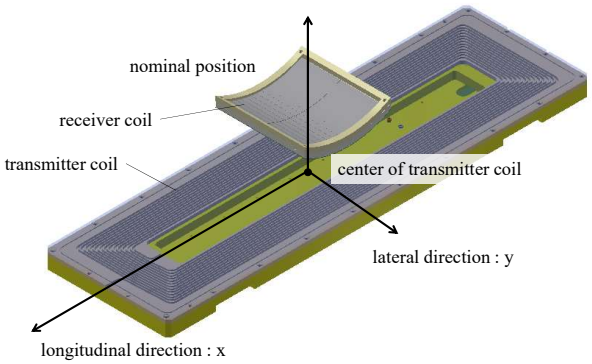

Fig. 9. Coil Position of Evaluation for Coil Parameters

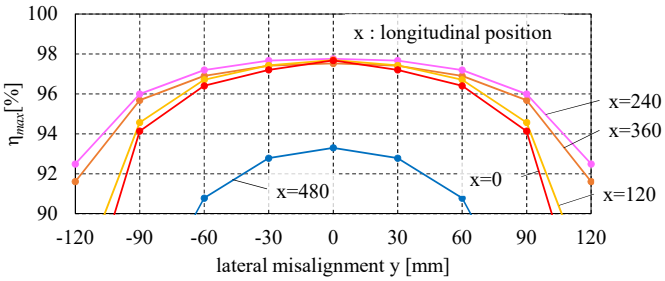

Fig. 10. η_{max} vs. lateral position of the receiver coil with each longitudinal position

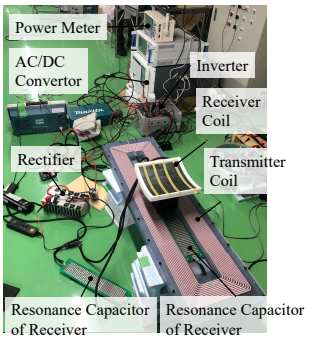

Fig. 11. WPT test bench

output of the receiver are connected to same converter. Thus equivalent load is not optimized into maximum efficiency. The capacitor of the transmitter is 14.0nF and the capacitor of the receiver is 39.4nF. Then test frequency is set 84.7kHz.

The evaluation result is depicted in Fig. 12 and Fig. 13. The output reaches 10.8kW and DC to DC efficiency which includes inverter loss, coil loss and rectifier loss is 91.6 % with 300V input. When converted to one car, the output is 21.6kW(two wheels) or 43.2kW(4 wheels).

VI. Evaluation of the WPT Loss Due to the Wheel

A. Evaluation by Test Bench

The WPT loss due to the wheel material is evaluated. In the proposed system, the wheel is located between the WPT coils, and is generally composed of iron or aluminum. Therefore, eddy current loss occurs in the wheel decreasing the efficiency and output. This eddy current loss is expressed by the following equation:

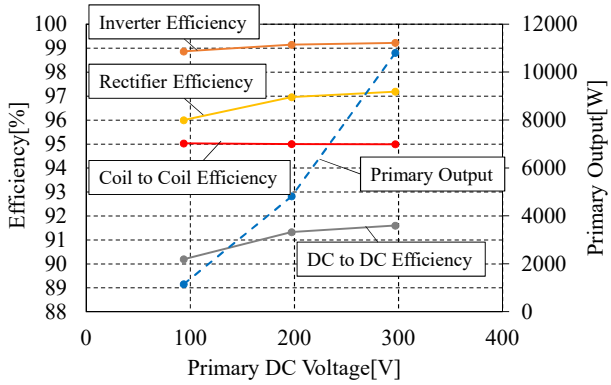

Fig. 12. Measured values at WPT bench, power vs. dc voltage and efficiency vs. dc voltage

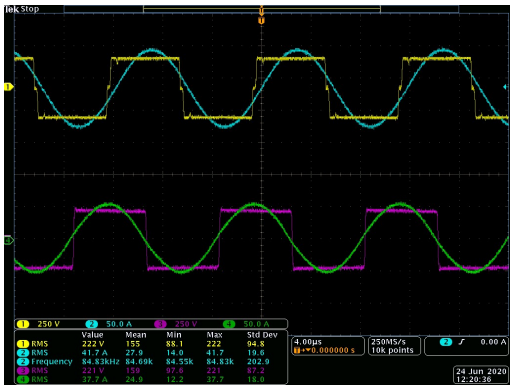

Fig. 13. Waveform of voltages and currents with 300V input, yellow: voltage of the transmitter side(250V/div), blue: current of the transmitter side(50A/div),purple: voltage of the receiver side(250V/div), green: current of the receiver side(50A/div)

$$P_{eddy} = \frac{x(\omega B_m)^2}{\rho} \tag{13}$$

Here, P_{eddy} is the eddy current loss, x is a parameter determined by the material shape and skin effect, ω is the frequency, B_m is the magnetic flux, and ρ is the material electric resistivity. Eddy currents not only cause loss but also resonant frequency shifts resulting in system decoupling and efficiency decrease.

The influence of the tire on the WPT system is verified using the characteristic evaluation equipment shown in Fig. 14, with an LCR meter. The evaluation frequency is 85 kHz as per the SAE J2954 standard.

The evaluated materials include iron, aluminum, and two types of CFRP which are applied in commercialized wheels. The dimensions of the test pieces are width 150mm, depth 150mm,and height 6mm.

Although the same carbon fiber is used for both the CFRP types, the knitting methodology differs;

One is a cross CFRP, whereas the other is unidirectional (UD). The cross CFRP, which is isotropic, is knitted similar to clothes; the UD CFRP, which is anisotropic, is only bundled. As the UD CFRP has stronger directional strength than the

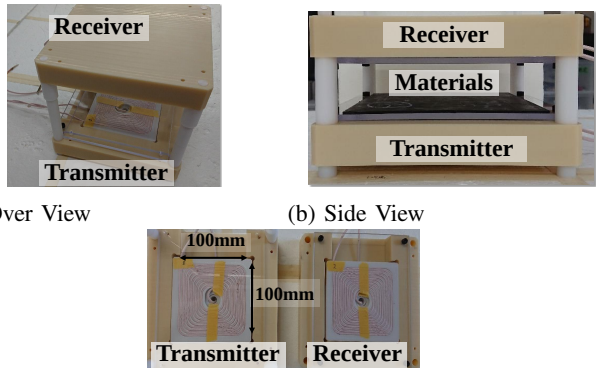

(a) Over View (b) Side View

(c) Coil Dimension

Fig. 14. Material evaluation equipment, materials set between small scale coils

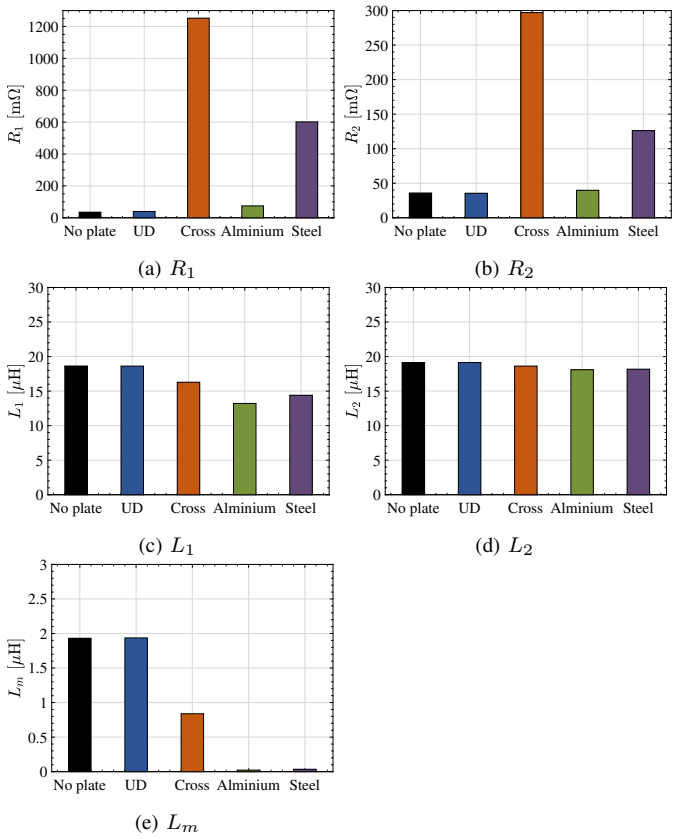

(a) R_1 (b) R_2

(c) L_1 (d) L_2

(e) L_m

Fig. 15. Measured values of the wheel material test with material evaluation equipment

cross CFRP. The specification of carbon fiber is shown in Table. V.

The carbon fiber has slight conductivity [18], and is therefore, impregnated with insulation resin. Hence, the DC resistance of the CFRP plate cannot be measured because of this resin courting. Thus, it is impossible to predict its eddy current loss using a DC resistance tester.

On the other hand, using CFRP as electro field shield [19] is studied with numerical model. As other approach, electric characteristic of CFRP is estimated with high frequency excitation coil and temperature obtained by thermo camera [20]. The measured values of the wheel material are depicted in

TABLE V
SPECIFICATIONS OF THE CARBON FIBER FOR CROSS AND UD CFRP

Parameter	Value
Tensile strength[MPa]	4900
Density[g/cm^3]	1.8
Diameter[μm]	7

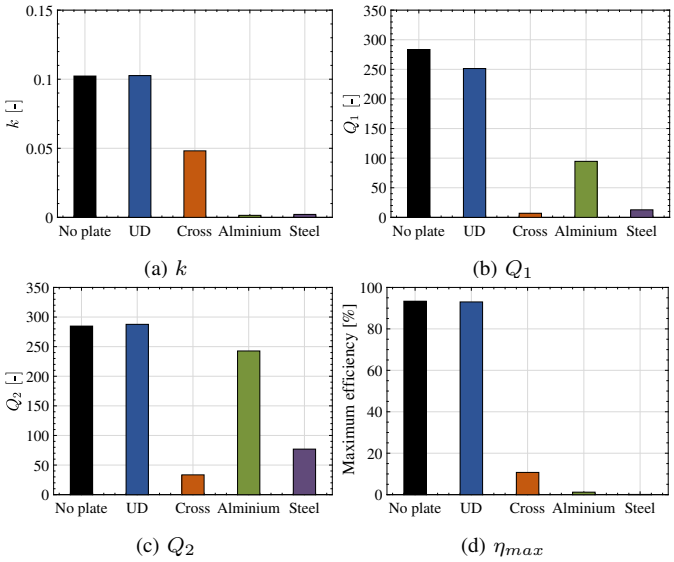

(a) k (b) Q_1

(c) Q_2 (d) η_{max}

Fig. 16. Calculated values of the wheel material test based on actual measurement

Fig. 15, whereas the calculated ones are shown in Fig. 16.

Both aluminum and iron affect the WPT efficiency critically. The skin effect is a major factor because L_m is almost zero for metals.

In addition, the cross CFRP affects the WPT efficiency critically. L_m of the cross CFRP is approximately half of the test result of that without any material. The skin effect is less than in metal materials; however, the eddy current loss increases because of the skin depth.

On the other hand, the UD CFRP hardly affects the WPT efficiency. There is a slight increase in R_1 and R_2, whereas the changes in L_1,L_2, and L_m are negligible because of the CFRP. The carbon fibers in the cross CFRP are in contact with each other because of the knitting; on the other hand, the carbon fibers in the UD CFRP are not in contact. Only minor eddy currents may be generated in the UD CFRP because its resin well isolates each carbon fiber. Moreover UD CFRP is better for application in products whose stress is concentrated in one direction, such as a wheel rim. Comparison of UD CFRP composite plate and aluminum plate is shown in Table VI. Parameters of UD CFRP composite plate are obtained when fiber lamination direction is 0 degree which has highest strength.

UD CFRP has more than ten times tensile strength, even though density is 60%. Thus, the most suitable material for the wheel of the in-wheel coil is the UD CFRP.

B. Evaluation for Resistivity by FEM Model

Wheel materials are also evaluated by finite element method(FEM) model, because resistivity of CFRP plate can

TABLE VI
SPECIFICATIONS OF UD CFRP COMPOSITE PLATE AND ALUMINUM PLATE

Parameter	Value	
	UD CFRP	Aluminum
Tensile strength[MPa]	2910	260
Density[g/cm^3]	1.57	2.69
Elongation[%]	2.15	10.0

not be measured directly. In this study, resistivity of the inserted plate between the transmitter and receiver coil is changed and mutual inductance of the coils is calculated. The dimensions of the FEM model is the same as material evaluation equipments. The result of calculation at 85kHz is shown in Fig. 17.

The mutual inductance saturates toward the upper limit at about $10^{-3}\Omega$m. That means equivalent resistivity of UD CFRP plate is over $10^{-3}\Omega$m. There is 4% of error between actual measurement data and the result of FEM due to accuracy of the calculation model. Though, according to the result of FEM, equivalent resistivity of cross CFRP plate is $1.2\text{x}10^{-5}\Omega$m, it is considered that actual equivalent resistivity is $1.15\text{x}10^{-5}\Omega$m. Resistivity of evaluated aluminum is $4.92\text{x}10^{-8}\Omega$m, thus this cross CFRP plate does not have low resistivity like metal.

VII. EVALUATION OF THE WPT LOSS DUE TO THE TIRE

Furthermore, the WPT loss due to the tire is evaluated. In the proposed system, the tire is located between the WPT coils. As a basic test, four representative types of rubber are evaluated because the conductivity of rubber is less and it varies [21]. The four characteristic types of rubber used are listed in Table. VII.

The evaluation equipment for rubber is same as that used for the wheel material. The calculated values of the evaluated rubber based on the measured values are displayed in Fig. 18.

No changes in the WPT efficiency are observed for any type of rubber. Further, the tire tread comprising the steel belt and rubber is evaluated. The steel belt inserted in the center of tire affects the WPT performance [22]. Therefore, in the worst case, inductive heating by the eddy current not only results in loss but also causes fire in the rubber.

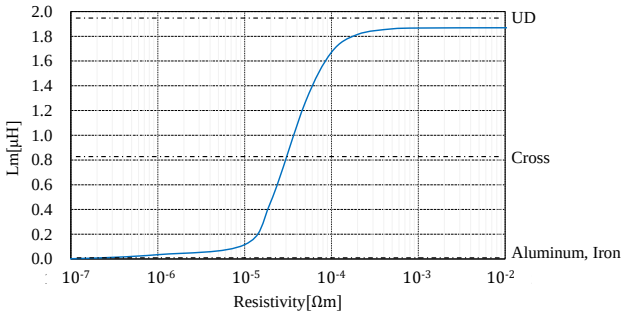

Fig. 17. FEM result by changing resistivity of the inserted plate: blue line shows calculated data, and black dash-dotted line shows actual measurement data of mutual inductance

TABLE VII
CHARACTERISTICS OF THE EVALUATED RUBBER

No.	1	2	3	4
Car type	Passenger car		Truck	
Use type	Sports	Eco	Sports	Eco

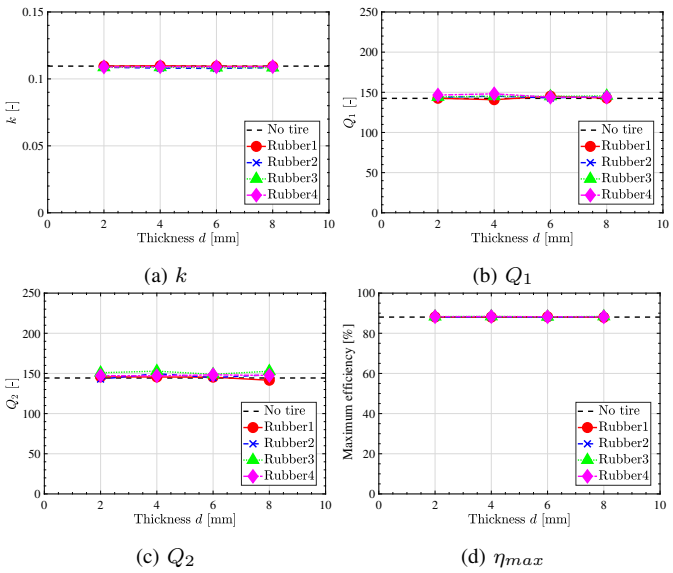

Fig. 18. Calculated values of the rubber test based on actual measurement with the material evaluation equipment

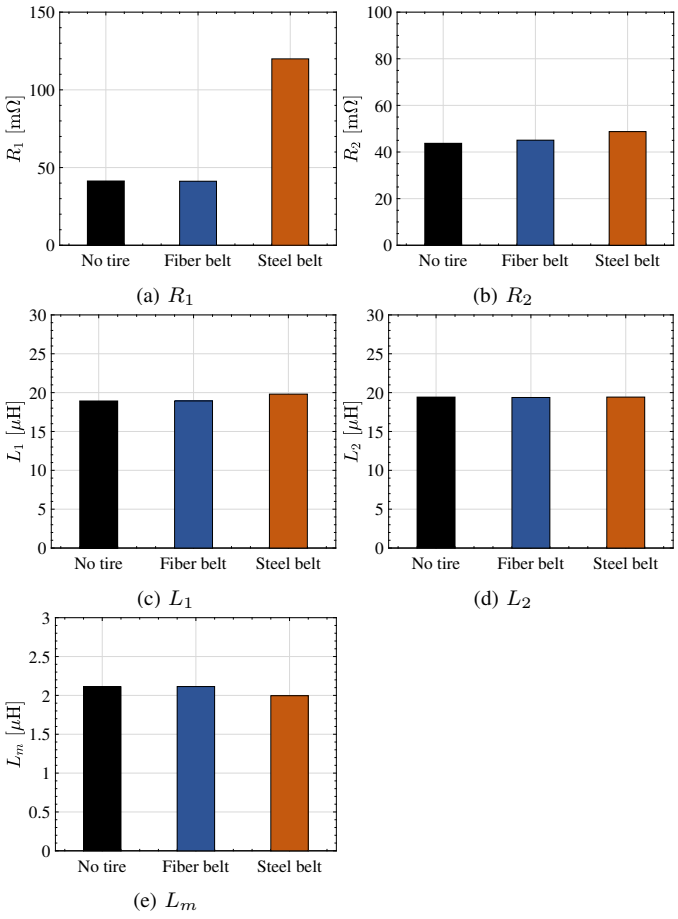

Fig. 19. Measured values of the tread part test with the material evaluation equipment

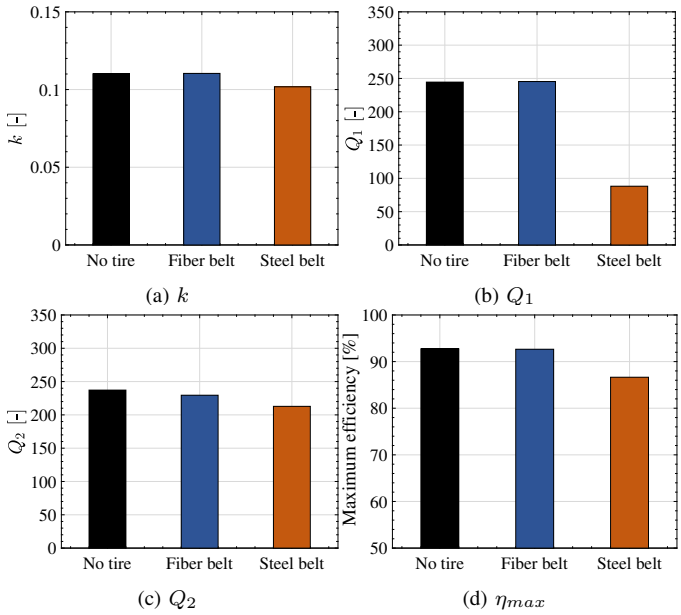

Fig. 20. Calculated values of the tread test based on actual measurement

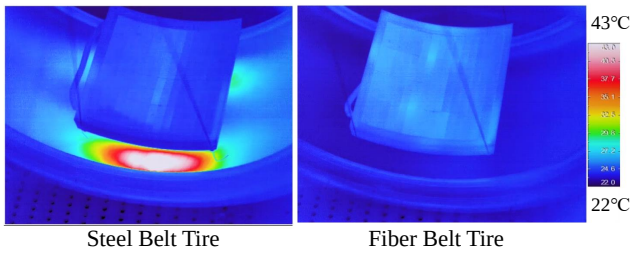

Fig. 21. Temperature of parts at the end of WPT test : the highest temperature point in steel belt tire is a part of belt

To solve this problem, a fiber belt with no conductivity is proposed. Such fiber belts have already been adopted for airplane tires. The measured values of the tread are shown in Fig. 19, and the calculated values using the measured values are shown in Fig. 20.

R_1 of the steel belts is thrice as no tires, and steel belts occurs about twice bigger WPT loss. As expected, it is confirmed that the fiber belts do not affect the WPT efficiency. Finally, thermal test is done with 20 inch fiber belt tire and full scale coil. The equipments for the test are same as Fig. 11. Temperature of the tire is evaluated by thermal camera. Tire is set between the transmitting coil and the receiving coil. Test frequency is 85 kHz and DC voltage is 90V. The test result 15sec after transmitting start is shown in Fig. 21. The temperature rise of iron belt tire is 20 °C, against that the temperature rise of fiber belt tire is not at all. Thus, the most suitable material for the tire of the in-wheel coil is the fiber belt.

VIII. Conclusion

In this study, a novel method for a dynamic WPT system, and suitable materials for its wheel and tire were proposed. The proposed system can reduce the possibility of foreign-object entry between the transmitter and receiver coils. In addition, a corresponding mutual inductance model was proposed.

The conclusions on the coil design are as follows:

1) The error between the calculations using a model and the actual measurement is $\pm 5\%$, when evaluated with a full- scale model.
2) An arc-shaped coil has more mutual inductance than a rectangular coil because of its small air gap.
3) The arc-shaped coil can achieve 10.8kW output per wheel with 91.6% DC to DC efficiency.

The major findings regarding the material for the wheel and tire are as follows:

1)UD CFRP is the most suitable material for the wheel because of its low loss.
2)Rubber does not affect the WPT efficiency at 85kHz.
3)The fiber belt is the most suitable belt for the tire because of its low loss

CFRP and fiber belt have been focused for light weighting or its high strength, however this research revealed other benefits that is suitable for WTP because of its low loss.

In future, we intend to evaluate more output and adjust control and achieve more efficiency. We will design the 1/1 scale UD CFRP wheel with the fiber tire and evaluate as whole WPT system as the future work. The air gap of the transmitter and receiver coils, which effects efficiency critically, of proposed system depends on radius of tire and thickness of wheel and tire. Since the dimensions of wheel and tire are given by market products in this research, efficiency will be improved by redesigning of wheel and tire for in-wheel coil. This system can allow for a misalignment as wide as the width of the tire because coil width is less than width of tire when the width of the transmitter coil is the same as the receiver. Therefore autonomous driving or driver assistance system is helpful for this system.

Acknowledgment

This work was partly supported by JSPS KAKENHI Grant Number 18H03768, JST CREST Grant Number JPMJCR15K3, and JST-Mirai Program Grant Number JPMJMI17EM, Japan.

References

[1] G.Covic, J.Boys, M.Kissin, H.Lu “A three-phase inductive power transfer system forroadway-powered vehicles”, *IEEE Transactions on Industrial Electronics*, vol.54, no.6, pp. 3370-3378, November 2007
[2] J.Huh, S.Lee, W.Lee, G.Cho, C.Rim “Narrow-Width Inductive Power Transfer System for Online Electrical Vehicles”,IEEE Transactions on Power Electronics, vol.26, no.12, pp. 3666-3679, June 2011
[3] O.Onar, J.Miller, S.Campbell, C.Coomer, C.White, L.Seiber “A Novel Wireless Power Transfer for in-motion EV/PHEV Charging”, 2013 Twenty-Eighth Annual IEEE Applied Power Electronics Conference and Exposition (APEC)
[4] L.Zhao, D.Thrimawithana, U.Madawala “Hybrid Bidirectional Wireless EV Charging System Tolerant to Pad Misalignment”, *IEEE Transactions on Industrial Electronics*, vol.64 ,no.9, pp.7079 - 7086, March 2017
[5] Z. Zhou, L. Zhang, Z. Liu, Q. Chen, R. Long and H. Su, “Model Predictive Control for the Receiving-Side DC-DC Converter of Dynamic Wireless Power Transfer”, *IEEE Transactions on Power Electronics*, vol.35, no.9, pp.8985-8997, September 2020
[6] R. Tavakoli and Z. Pantic, “Analysis, Design, and Demonstration of a 25-kW Dynamic Wireless Charging System for Roadway Electric Vehicles”, *IEEE Journal of Emerging and Selected Topics in Power Electronics*, vol.6, no.3, pp.1378-1393, September 2018

[7] O. Shimizu, S. Nagai, T. Fujita, H. Fujimoto: "Potential for CO2 Reduction by Dynamic Wireless Power Transfer for Passenger Vehicles in Japan ", *Energies 2020*, 13, 3342, Jun. 2020

[8] H.Fujimoto, T.Takeuchi, K.Hanajiri, K.Hata, T.Imura, M.Sato, D.Gunji, G.Guidi "Development of Second Generation Wireless In-Wheel Motor with Dynamic Wireless Power Transfer", The 31st International Electric Vehicle Symposium & Exhibition and International Electric Vehicle Technology Conference 2018

[9] A.Mohamed, C.Lashway, O.Mohammed "Modeling and Feasibility Analysis of Quasi-Dynamic WPT System for EV Applications", *IEEE Transactions on Transportation Electrification*, vol.3 ,no.2, pp.343-353, March 2017

[10] B.Limb, T.Bradley, B.Crabb, R.Zane, C.McGinty, J.Quinn "Economic and Environmental Feasibility, Architecture Optimization, and Grid Impact of Dynamic Charging of Electric Vehicles using Wireless Power Transfer", 6th Hybrid and Electric Vehicles Conference (HEVC 2016)

[11] D.Gunji, K.Hata, O.Shimizu, T.Imura, H.Fujimoto "Feasibility Study on In-motion Wireless Power Transfer System Before Traffic Lights Section", 2019 IEEE PELS Workshop on Emerging Technologies: Wireless Power (WoW)

[12] J.Chakarothai, K.Wake, T.Arima, S.Watanabe, T.Uno "Exposure Evaluation of an Actual Wireless Power Transfer System for an Electric Vehicle With Near-Field Measurement", *IEEE Transactions on Microwave Theory and Techniques*, vol.66 ,no.3, pp.1543-1552, September 2017

[13] T.Imura "Simple equivalent circuit model with foreign object on wireless power transfer via magnetic resonant coupling", 2017 IEEE Conference on Antenna Measurements & Applications

[14] O.Shimizu, T.Imura, H.Fujimoto, D.Gunji, K.Akutagawa and G. Guidi, "Mutual Inductance Modeling of In-Wheel Arc-Shaped Coil for In-Motion WPT", 2019 IEEE Wireless Power Transfer Conference (WPTC), London, United Kingdom, 2019, pp.624-628,

[15] P.Zhang, Q.Yang, X.Zhang, Y.Li, Y.Li "Comparative Study of Metal Obstacle Variations in Disturbing Wireless Power Transmission System", *IEEE Transactions on Magnetics*, vol.53, no.6, pp.1-4, June 2017

[16] G.Wasselynck, D.Trichet, B.Ramdane, J.Fouldagar "Interaction Between Electromagnetic Field and CFRP Materials: A New Multiscale Homogenization Approach", *IEEE Transactions on Magnetics*, vol.46, no.8, pp.3277-3280, August 2010

[17] Y.Cheng, Y.Shu "A New Analytical Calculation of the Mutual Inductance of the Coaxial Spiral Rectangular Coils", *IEEE Transactions on Magnetics*, vol.50, no.4, pp. 1-6, April 2014

[18] C.Holloway, M.Sarto, M.Johansson "Analyzing Carbon-fiber Composite Materials with Equivalent-layer Models", *IEEE Transactions on Electromagnetic Compatibility*, vol.47, no.4, pp. 833 - 844, November 2005

[19] T.Campi, S.Cruciani, V.De Santis, F.Maradei, M.Feliziani, "Numerical Calculation of the Near Field Shielding for Carbon Fiber Reinforced Polymer (CFRP) Panels at Wireless Power Transfer Automotive Frequencies", 2018 IEEE Symposium on Electromagnetic Compatibility, Signal Integrity and Power Integrity (EMC,SI&PI), Long Beach, CA,2018, pp.444-447.

[20] H.K.Bui, F.D.Senghor, G.Wasselynck, D.Trichet, J.Fouladgar, K.Lee, G. Berthiau, "Characterization of Electrical Conductivity of Anisotropic CFRP Materials by Means of Induction Thermography Technique", *IEEE Transactions on Magnetics*, vol. 54, no.3, pp.1-4

[21] L.Boca "Influence of the magnetic field on the electric conductivity of magnetorheological elastomers", *Journal of Industrial and Engineering Chemistry*, vol.16, no.3, pp.359-363, May 2010

[22] C.Panchal, J.Lu, S.Stegen "Static In-wheel Wireless Charging Systems for Electric Vehicles",*International journal of scientific & technology research*, vol.6, no.09, September 2017

Osamu Shimizu (M'19) received the B.S. and M.S. degrees in Faculty of Environment and Information Studies from Keio University, Japan in 2007 and 2009,respectively. He worked as an associate at Toyota Motor Corporation, Sim-Drive Co., Ltd., Honda R & D Co., Ltd.in 2009-2017. He received the Ph.D. degree in the Department of Media and Governance from Keio University in Japan. He joined as an assistant professor at Nagoya University in 2017. From 2018. He joined Graduate School of Frontier Science at University of Tokyo as a project assistant professor. His interest are in design and control of electric vehicle driving system and WPT system. He is a member of IEEE, IEE and the Society of Automotive Engineers of Japan.

Takashi Utsu (S'19) received the B.S.degree in Department of Applied Physics from Tokyo University of Sience, Tokyo, Japan in 2018. He is currently a Research Student in The University of Tokyo, Kashiwa, Japan. His interest are in design of WPT system and magnetic circuit.

Hiroshi Fujimoto (S'99-M'01-SM'13) received the Ph.D. degree in the Department of Electrical Engineering from the University of Tokyo in 2001. In 2001, he joined the Department of Electrical Engineering, Nagaoka University of Technology, Niigata, Japan, as a research associate. From 2002 to 2003, he was a visiting scholar in the School of Mechanical Engineering, Purdue University, U.S.A. In 2004, he joined the Department of Electrical and Computer Engineering, Yokohama National University, Yokohama, Japan, as a lecturer and he became an associate professor in 2005. He is currently an associate professor of the University of Tokyo since 2010. He received the Best Paper Awards from the IEEE Transactions on Industrial Electronics in 2001 and 2013, Isao Takahashi Power Electronics Award in 2010, and Best Author Prize of SICE in 2010. His interests are in control engineering, motion control, nano-scale servo systems, electric vehicle control, and motor drive. He is a senior member of IEE of Japan and IEEE. He is also a member of the Society of Instrument and Control Engineers, the Robotics Society of Japan, and the Society of Automotive Engineers of Japan.

Daisuke Gunji (M'13) received the B.S. and M.S. degrees in mechanical engineering and intelligent systems from The University of Electro- Communications, Tokyo, Japan in 2005 and 2007,respectively. In 2007, he joined NSK Ltd, Kanagawa,Japan. He received the Ph.D. degree in the Graduate School of Frontier Sciences, The University of Tokyo, Chiba, Japan, in 2015. His research interests include wireless power transfer, motion control, and electric vehicle control. He is a member of the Institute of Electrical Engineers of Japan, the Society of Automotive Engineers of Japan.

Isao Kuwayama received the B.E. and M.E. degree in mechanical engineering from the University of Waseda, in 1997 and 1999. After that, he joined Bridgestone Corporation as a member of Tire Research Department and started his career as a tire researcher from 1999. He received Ph.D. degree in mechanical engineering from the Politecnico di Milano in 2008 and returned to Bridgestone and currently works as a chief researcher of Next Generation Technology Development Department. His research interests cover the tire/vehicle dynamics, measurement system, computational mechanics, and so on.